Supplemental Material:

Interactions for Seamlessly Coupled Exploration of High-Dimensional Images and Hierarchical Embeddings

A. Vieth, A. Vilanova, B. Lelieveldt, E. Eisemann, and T. Höllt

S0: Background - Hierarchical Embeddings

A *hierarchical embedding* method typically extends existing DR techniques by creating a hierarchical representation of the original data items and projecting only elements from individual hierarchy levels instead of all data [NA19][†]. Using the notation for hierarchical embeddings from Höllt et al. [HVP*19], the hierarchical data structure consists of *landmarks*, within m levels, namely the sets $\mathcal{L}^0 \dots \mathcal{L}^{m-1}$. The lowest hierarchy level $\mathcal{L}^0$ contains all data points. Each landmark $L_i^{k+1} \in \mathcal{L}^{k+1}$ in a higher hierarchy level represents ($\rightarrow$) a set of landmarks from the lower level $\mathcal{L}^k = \{L_i^k \mid L_i^k \leftarrow L_j^{k+1}\}$. Thus, the higher embedding levels provide more abstract representations of the original data. Here, for simplicity, we assume the hierarchy to be a proper tree: each landmark L_i^k is represented by only one landmark in $\mathcal{L}^{k+1}$. In practice this is not necessarily the case [PHL*16].

Given a selection of landmarks $\mathcal{S}^k$ on a level k, we are interested in their relation to landmarks in other hierarchy levels. Following the terminology for visualizations of hierarchically structured data from Elmqvist et al. [EF10], we describe coarsening the level of detail, i.e., the process of finding all landmarks $\mathcal{S}^{k+1}$ on the more abstract level $k+1$ that well represent them, as *rolling-up*. Analogously, refining the level of detail, that is finding the landmarks $\mathcal{S}^{k-1}$ on the more detailed level $k-1$ that are represented by $\mathcal{S}^k$ is the result of *drilling-down*.

S1: Timings

Timings for regular HSNE and interactive HSNE, all taken on a machine equipped with an Intel Core i5-9600K CPU and a NVIDIA GeForce RTX 2080 SUPER GPU. The total embedding time is approximately equal to the data structure initialization and gradient descent time. Our hierarchy traversal step adds a comparably small overhead to the entire embedding computation. In most scenarios, the user is presented with iteratively updating embeddings within 300ms (hierarchy traversal plus data structure initialization times).

Table 1: Indian Pines: Durations of embedding update step connected to an image interaction. ROIs as indicated in Figure 4a. Times, in ms, are averages over 10 runs with sample standard deviation.

	ROI Ⓘ		ROI Ⓘⓘ		ROI Ⓘⓘⓘ	
Scale	2		2		3	
Landmarks	9,738		9,533		3,979	
Data points in view	57,424		58,212		50,691	
Hierarchy traversal [our]	48.0	(2.6)	39.3	(2.9)	39.2	(4.2)
Embedding	848.1	(78.2)	862.2	(17.8)	619.8	(33.2)
└ Data structure initialization	244.6	(11.8)	243.8	(4.7)	40.4	(2.5)
└ Gradient descent	598.8	(80.0)	614.0	(20.4)	545.5	(32.2)

Note: Times in ms, standard deviation in parentheses.

S2: Additional Indian Pines Information and Figures

The Indian Pines Test Site 3 [BBL15] data are a set of hyperspectral 145×145 pixel images with known class information for each pixel. This well analyzed data set is only a small part of a larger, unlabeled measurement of $614 \times 2,678 \approx 1.6$M pixels, depicting an area around the Purdue University Agronomy Center in Indiana, USA, made up of fields (e.g. corn and soy), forests, roads, rivers and houses. The pixel resolution is roughly 20m x 20m and contains electromagnetic spectral information from from 400 nm to 2400 nm sampled at 10 nm. We excluded 20 channels of the 220 channel data set due to their low information quality since they cover spectral water absorption bands, as suggested in [GC99]. This results in 200 samples, that we interpret as dimensions, forming our high-dimensional attribute space used as input for the dimensionality reduction. We normalized the data by clamping each channel to the 99.999th percentile and scaling it to the range [0, 1].

[†] Citations that were already mentioned in the main text are not listed again in the reference section at the end of this supplemental material.

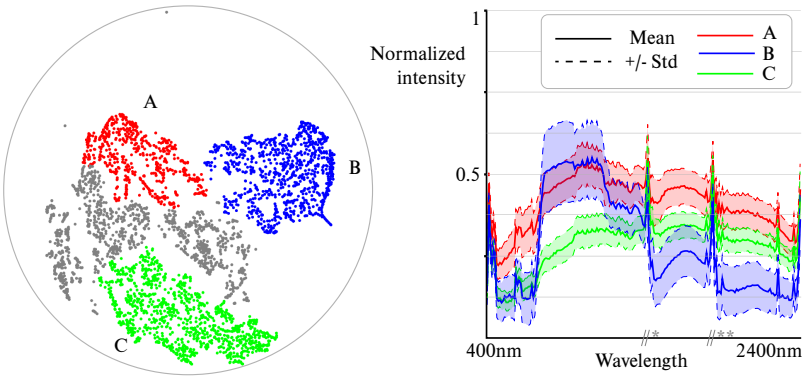

Figure 5: **Indian Pines cluster characteristics:** (a) shows the top level (4th) HSNE embedding of the Indian Pines data. (b) displays channel-wise intensity values for three cluster of different types of fields (A and C) and forest (B). * and ** indicate frequency bands that were omitted from the data. The three regions of interest discussed in Figure 4 are mostly represented with landmarks from the three clusters above.

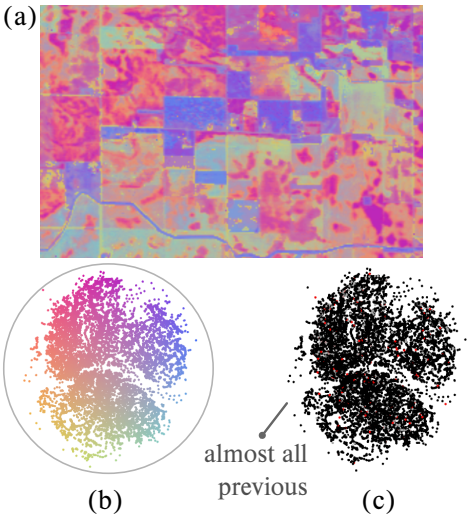

Figure 6: **Drill-down** of the embedding for ROI 3 from Figure 4d: the recolored image region (a), new embedding (b) and initializations (c).

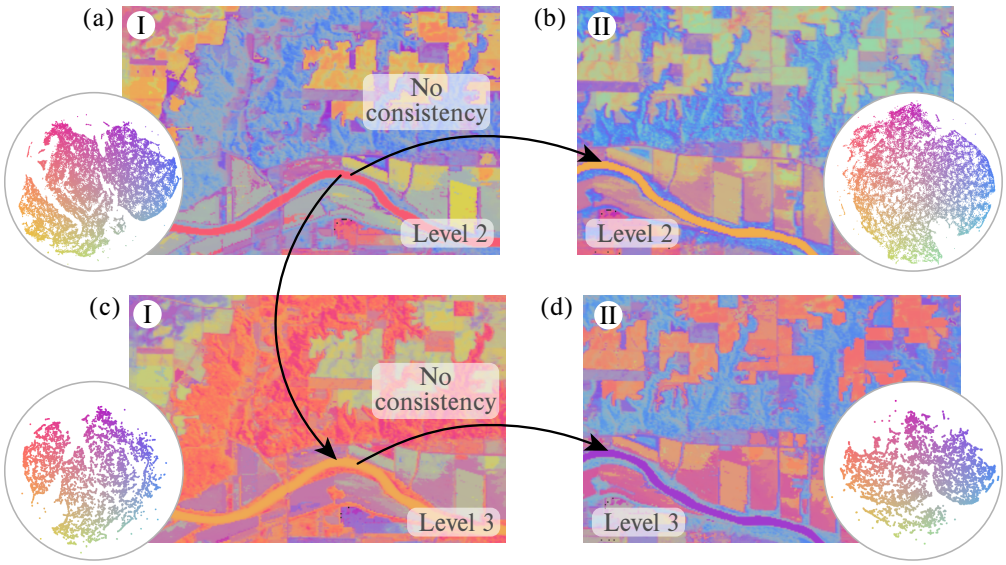

Figure 7: **Regular HSNE embeddings:** (a) and (b) as in Figure 4f and Figure 4g. (c) and (d) show the intermediate refinements on level 3 between the top level embedding and the level 2 embeddings. They contain 11,857 and 11,207 landmarks respectively while the level 2 embeddings contain 50,116 and 46,461 landmarks respectively.

References

[GC99] GUALTIERI J. A., CROMP R. F.: Support Vector Machines for Hyperspectral Remote Sensing Classification. In *27th AIPR Workshop: Advances in Computer-Assisted Recognition* (1999), vol. 3584, SPIE, pp. 221–232. doi:10.1117/12.339824. 1